CELL & GENE THERAPY INSIGHTS

RESEARCH ARTICLE

Successful *ex vivo* expansion of pro-angiogenic cells from one single primitive hematopoietic stem cell identifies a novel tactic for treatment of limb ischemia

Atsuhiko Oikawa*, Giuseppe Mangialardi*, Jai Richards, David Ferland-McCollough, Iker Rodriguez-Arabaolaza, Rajesh G Katare, Sophie E Mansell & Paolo Madeddu

Objective: Bone marrow cell therapy has pioneered the field of regenerative medicine for the treatment of ischemic disease, but remains a controversial topic due to persistent uncertainty on purity and quality of the cell product. Here, we evaluated the therapeutic activity of pro-angiogenic clones derived from single-sorted long-term repopulating hematopoietic stem cells (LT-HSCs, $CD150^+/CD34^-/Lineage^-/Sca\text{-}1^+/c\text{-}Kit^+$) in a murine model of hindlimb ischemia. **Approach and Results:** C57BL/6 mice underwent unilateral limb ischemia by femoral artery occlusion, followed by intramuscular injection of green fluorescent BM LT-HSCs cells (2,000 per mouse) from congenic donor C57BL/6-Tg(CAG-EGFP)131Osb/LeySopJ mice or vehicle (PBS). Cell therapy with LT-HSCs markedly accelerated the recovery of blood flow to the ischemic limb as measured by laser Doppler flowmetry ($P<0.05$ vs. vehicle). LT-HSC-injected muscles showed increased capillary (577±67 vs. 374±35/mm^2, $P<0.05$) and arteriole density (108 ±6 vs. 72 ±9/mm^2, $P<0.05$). Additionally, LT-HSC therapy improved the viability and proliferation of resident vascular cells. In separate experiments, single sorted BM LT-HSC-derived cells were expanded up to 40,000 fold in culture giving rise to two distinct clone subsets, according to the expression level of the surface marker CD31. Upon transplantation in the mouse ischemic model, $CD31^{high}$ LT-HSC-derived cells showed superior pro-angiogenic and pro-healing activities as compared with $CD31^{low}$ LT-HSC-derived cells. **Conclusions:** These data establish clonogenic $CD31^{high}$ LT-HSC-derived cells as a promising cell therapy approach for the treatment of limb ischemia. *Authors contributed equally to this paper

Submitted for review: Dec 2 2015 ▶ **Revised Accepted:** Apr 20 2016

Critical limb ischemia (CLI), the end stage of peripheral artery disease (PAD), is caused by severe obstruction of blood flow resulting in unbearable pain, ulcers, and high risk for amputation [1]. Surgical bypass or percutaneous revascularization, the gold standard for the treatment of CLI, exert only temporary symptomatic alleviation. Furthermore, around one third of patients with CLI cannot be revascularized because of multivascular disease or occlusions of small-caliber blood vessels [2,3]. Gene and cell therapies have been therefore proposed as a possible complement or alternative to interventional angioplasty [4].

Clinical trials using bone marrow (BM)-derived cells showed significant therapeutic benefit, including improvement of ankle brachial index, transcutaneous partial pressure of oxygen, pain relief, and decreased risk of amputation [5]. However, despite initial evidence of safety and efficacy, BM cell therapy remains a controversial topic due to the lack of unambiguously defined isolation protocols, delineation of differentiation hierarchy and quality/quantity standards. Furthermore, the seminal concept of BM cells directly participating in *de novo* post-natal vasculogenesis, proposed some years ago by Asahara *et al.*, have been revised in light of the novel indication that paracrine mechanisms, rather than the conversion of one cell type to another, are responsible for reciprocal interactions between hematopoietic and vascular cells within the BM microenvironment as well as after transplantation in peripheral tissues [6–9]. In line, BM vascular cells are able to recreate the hematopoietic microenvironment following transplantation at heterotopic sites, through the release of angiopoietin-1 and activation of the Notch signaling pathway [10,11]. Reciprocally, hematopoietic cells promote neovascularization of peripheral tissues principally through the release of soluble and packaged angiogenic factors [12,13].

Initial evidence suggests that pro-angiogenic cells (PACs) are particularly enriched in the fraction of multipotent long-term repopulating hematopoietic stem cells (LT-HSCs), which in the mouse are identified as $CD34^-$/c-Kit^+/$Sca\text{-}1^+$/$Lineage^-$ ($CD34^-$/KSL) cells [14]. However, $CD34^-$/KSL cells represent a heterogeneous population containing sub-fractions with diverse regenerative capacity. Further characterization by use of the Signaling Lymphocyte Activation Molecule (SLAM) marker CD150 allows identification of a fraction of $CD34^-$/KSL cells endowed with high self-renewal potential and repopulating capacity [14,15]. It remains unknown however if the same approach may be useful to establish a pro-angiogenic hierarchy within the population of LT-HSCs.

We propose that the CD150 marker may help select proper PACs from the bulk population of $CD34^-$/KSL cells and that transplantation of small dosage $CD150^+$/$CD34^-$/KSL cells may benefit the healing of ischemic limbs. Results confirm the presence of clonogenic PACs in the mouse BM $CD150^+$/$CD34^-$/KSL cell fraction. Additionally, we discovered that $CD31^{high}$-expressing clones derived from single sorted $CD150^+$/$CD34^-$/KSL cells possess superior and more durable pro-angiogenic and pro-survival activities *in vivo*. Our refined approach provides new impetus to BM cell therapy for the treatment of CLI.

MATERIALS & METHODS

Ethics

Experiments were performed in accordance with the *Guide for the Care and Use of Laboratory Animals* (the Institute of Laboratory Animal Resources, 1996) and with approval of the British Home Office and the University of Bristol.

Isolation of $CD150^+$/$CD34^-$/KSL HSCs

Bone marrow was extracted from 10–12-week-old male C57BL/6

DOI: 10.18609/cgti.2016.019

(Harlan, UK) mouse tibia and femur. A total of six mice were used per isolation. Total BM cells were washed with ice-cold Hank's balanced salt solution containing 0.5% bovine serum albumin and 0.02% sodium-azide. Cells were resuspended and stained in this buffer with anti-Lineage mixture (Biotin, Miltenyi Biotec, Germany) anti Sca-1 (PE, eBioscience, CA USA), anti c-Kit (APC-eFluor 780, eBioscience), anti-CD34 (Alexa-Fluor 700, eBioscience) and anti CD150 (APC, eBioscience). Streptavidin-PE-Cy7 conjugated antibodies were used as secondary for anti-Lineage mixture.

Flow cytometry analysis

To identity surface markers on KSL-selected and clonogenically expanded cells, fluorescence activated cell sorting (FACS) analysis was performed. Surface expression of mouse Flk-1, CD31, Tie-2 and c-Kit were determined using a PE-conjugated anti Flk-1 (BD Biosciences, CA, USA), BV421-conjugated anti CD31 (BD), APC-conjugated anti Tie-2 and APC-eFluor 780-conjugated anti c-Kit (eBioscience). Flow cytometry was performed on a FACSCalibur (BD) equipped with FACSDiva software (BD).

Hindlimb ischemia model & cell transplantation

Male 10–12-week-old C57BL/6J mice (Harlan) underwent unilateral hindlimb ischemia by ligature of the proximal end of the femoral artery. Immediately after ischemia induction, 2,000 GFP^+, $CD150^+/CD34^-$/KSL cells from congenic mice or vehicle (PBS, 30 μL) were injected into three different points of the ischemic adductor muscle (n = 6 animals per group). A second set of experiments were performed comparing clonogenically expanded $CD150^+/CD34^-$/KSL cells, according to levels of CD31 expression: three groups were studied, with mice randomized to receive $CD31^{high}/CD150^+/CD34^-$/KSL or $CD31^{low}/CD150^+/CD34^-$/KSL cells or vehicle (n = 5 animals per group). Blood flow recovery was followed up by laser Doppler flowmetry at day 3, 7 and 21. The Doppler data were normalized as the mean ratio of ischemic to contralateral limb measurements.

Source of labelled BM-HSCs for cell tracking after *in vivo* transplantation

Donor BM-HSCs were obtained as described above from male 10–12 week-old C57BL/6J (Harlan) GFP congenic mice (C57BL/6-Tg (CAG-EGFP) 10sb/J) (The Jackson Laboratory, ME, USA).

Evaluation of capillary & arteriolar density

At day 21, mice were perfused under physiologic pressure with paraformaldehyde 4% PBS. Adductor muscles were isolated and embedded in OCT. Capillary and arteriolar densities were assessed with the use of isolectin B4 (Invitrogen, UK) and α-smooth muscle actin (α-SMA; Sigma) staining as reported [16]. Briefly, histological sections of mouse adductor muscles were incubated for 1 hour at room temperature (RT) with biotin-conjugated isolectin B4 followed by Alexa-488 streptavidin-conjugated antibody (Invitrogen) to identify endothelial cells and Cy3-conjugated α-SMA to identify smooth muscle cells. Incubation with α-sarcomerin actin

(Sigma) followed by Alexa-568 secondary antibody (Invitrogen) was performed in order to identify myofibers. Slides were observed under a fluorescence microscope (Olympus CX41, Olympus, UK). Arterioles were distinguished from the capillaries and veins by the structure of tunica media in the vessel wall and the shape of the lumen. Isolectin-positive capillaries and α-SMA-positive arterioles were counted within 10 random fields per section (400x) (n = 5–9 animals per group). Results were expressed as capillary or arteriole to fiber ratio.

Assessment of apoptosis & proliferation

At Day 21, mice were perfused under physiologic pressure with paraformaldehyde 4% PBS. Adductor muscles were isolated and embedded in OCT. Histological cryosections were labelled by TUNEL in order to identify apoptotic cells. Briefly, 4% formaldehyde-fixed cryosections were pre-treated with proteinase K (1:50) for 15 min at RT. The TUNEL assay was performed using a TdT-Fluor *in situ* apoptosis detection kit (Trevigen, MD, USA). Sections were counterstained with DAPI to identify nuclei. Ten random fields from each section were captured (400x) for counting apoptotic cells (n = 5–9 animals per group). A counterstaining with biotin-conjugated isolectin B4 followed by Alexa-568 streptavidin-conjugated antibody (Invitrogen) was performed. TUNEL-positive cells with bright green nuclei were counted and expressed as numbers of TUNEL-positive nuclei over the total nuclei of positive lectin cells in the captured field. A treatment with TACS™ Nuclease (Trevigen) has been carried out as positive control.

Proliferating cells were identified by Ki67 staining. Briefly, 4% formaldehyde-fixed cryosections were incubated overnight at 4° C with rabbit anti-mouse Ki-67 antibody (Abcam, UK), followed by Alexa-488-conjugated anti-rabbit secondary antibody (Invitrogen) for 2 hours at room temperature. Counterstaining with biotin-conjugated isolectin B4 was followed by Alexa-568 streptavidin-conjugated antibody. Ten random fields were captured (400x) (n = 5–9 animals per group). Ki-67 positive cells with bright green nuclei were counted and expressed as numbers of Ki-67 positive nuclei over the total nuclei of positive lectin cells in the captured field.

Ex vivo expansion of single sorted $CD150^{+}/CD34^{-}$/KSL HSCs

A colony forming assay (CFA) was performed as previously described [17,18]. Single cells of mouse primitive LT-HSCs ($CD150^{+}/CD34^{-}$/KSL) were sorted into each well of a 96-well culture plate (Greiner bio-one, UK) using a Becton Dickinson Influx high speed cell sorter (BD). The sorted cells were cultured for 2 weeks in methylcellulose medium M3236 (Stem Cell Technologies, Canada) supplemented with 20 ng/ml Stem Cell Factor (SCF; R&D Systems, UK), 50 ng/mL VEGF (R&D Systems, UK), 20 ng/ml interleukin-3 (IL3; PeproTech, NJ, USA), 50 ng/mL Epidermal Growth Factor (EGF; PeproTech), 50 ng/mL Insulin-like Growth Factor-1 (IGF-1; PeproTech), and 2 U/mL heparin (Sigma).

DOI: 10.18609/cgti.2016.019

Real time (RT)-PCR to detect gene expression in cultured cells

RNA was extracted using the Trizol method (Thermo Fisher) using glycogen as a RNA carrier (Thermo Fisher). The extracted RNA was purified by acid phenol-chloroform phase separation and re-precipitated using isopropanol. The cDNA library was generated using 100 ng of isolated RNA, which underwent reverse-transcription by the High Capacity cDNA Reverse Transcription Kit (Thermo Fisher). Quantitative real-time PCR was performed using specific DNA primers (Sigma-Aldrich) and the Power Sybr reaction mix (Thermo Fisher) on the Light Cycler 480 II system (Roche Diagnostics, Switzerland) (Table 1). Expression was normalized to that of the housekeeping genes *GAPDH*.

Statistical analysis

All results are represented as mean ± SEM. Differences between multiple groups were compared by analysis of variance (ANOVA) followed by a Holm-Sidak multiple comparison test. Two-group analysis was performed by t-test (unpaired as appropriate).

RESULTS

Frequency of primitive HSCs

We first used flow cytometry to verify the relative abundance of primitive HSCs in murine BM. The frequency of $CD150^{+}/CD34^{-}$/KSL cells among total BM cells was around 0.002% ± 0.0002 (Figure 1A). Three independent sorting experiments were next performed. This allowed us to sort 1,500 to 2,500 $CD150^{+}/CD34^{-}$/KSL cells from total BM cells of a single mouse and then perform qRT-PCR for molecular characterization and *in vivo* transplantation in a model of limb ischemia (*vide infra*).

TABLE 1

Sequence of gene-specific primers used for qRT-PCR.

Primer	Sequence
Ang1 fwd	AAC CTC ACC CTG CAAAGATG
Ang1 rvs	CAC AGA TGG CCT TGA TGT TG
Ang2 fwd	CAAGGC ACTGAG AGACAC
Ang2 rvs	TGC GCT TCA GTC TGG TAC AC
VEGF fwd	TCTCCC AGATCG GTG ACAGT
VEGF rvs	GGG CAG AGC TGA GTG TTA GC
SCF fwd	AAC TATGTC GCC GGG ATG GA
SCF rvs	CTTCCATGC ATA ACA CGA GGTCA
SDF-1 fwd	CTG TAG CCTGAC GGACCAAT
SDF-1 rvs	CCA TTC TAC AGG AGG CCA AA
Tie2 fwd	TAC AAC GGC CAT TTC TCC TC
Tie2 rvs	GTG GCT TGC TTG GTA CAG GT
CXCR4 fwd	GCC AAG TTC AAAAGC TCTGC
CXCR4 rvs	AGC CTC TGC TCA TGG AGT TG
Thrombospondin1 fwd	GAA GTA CCC ACC TGC TTC CA
Thrombospondin1 rvs	TTT GGA GAG TGG ACC CAAAG
JAG1 fwd	AGA GAC AGG CAG GCG ATCT
JAG1 rvs	TGG GAT GCT TCC AAC TTC A
Dll1 fwd	CGG GAA AAA GAA AAC GTG TG
Dll1 rvs	ATA GAC CCG AAG TGC CTT TGT
Dll3 fwd	CTG GCC AGC CTA GAA CTC TG
Dll3 rvs	GAG TGG TGC ACG CCT TTA AT
Dll4 fwd	AGG CAA GAG TTG GTC CTT CC
Dll4 rvs	TTT AGC ATG AAG GCC CTG AG
Notch1 fwd	ATA GCA TGA TGG GGC CAC TA
Notch1 rvs	GGC AGG CCC TGG TAA ATA AT
Notch2 fwd	TTC CAG CTT ATC CCA AAA CG
Notch2 rvs	GGC ATC TCT GGG ATC TGG TA
Notch3 fwd	CTA GCC CAG CAA CTG CTA CC
Notch3 rvs	GGA ACA GAT ATG GGG TGT GG
Notch4 fwd	AAA TAA CCG TTA AGC TCA CTT GTC T
Notch4 rvs	GGT AGG CGA CAC TCG GTT CCC
GAPDH fwd	TGT GAA CGG ATT TGG CCG TA
GAPDH rvs	ACT GTG CCG TTG AAT TTG CC

Expressional profile of CD150^{+}/CD34^{-}/KSL cells

Stem cell factor (SCF, also known as c-Kit ligand) in concert with other cytokines and growth factors contributes to the self-renewal and maintenance of HSCs in the BM niche. Analysis of gene expression by RT-PCR indicates higher expression levels of SCF and the angiopoietin receptor Tie2 in CD150^{+}/CD34^{-}/KSL cells as compared to CD150^{-}/CD34^{-}/KSL cells (Figure 1B). In addition, the Notch signaling pathway represents a key mechanism in the regulation of HSC self-renewal and

FIGURE 1

Flow cytometry analysis of mouse BM LT-HSCs.

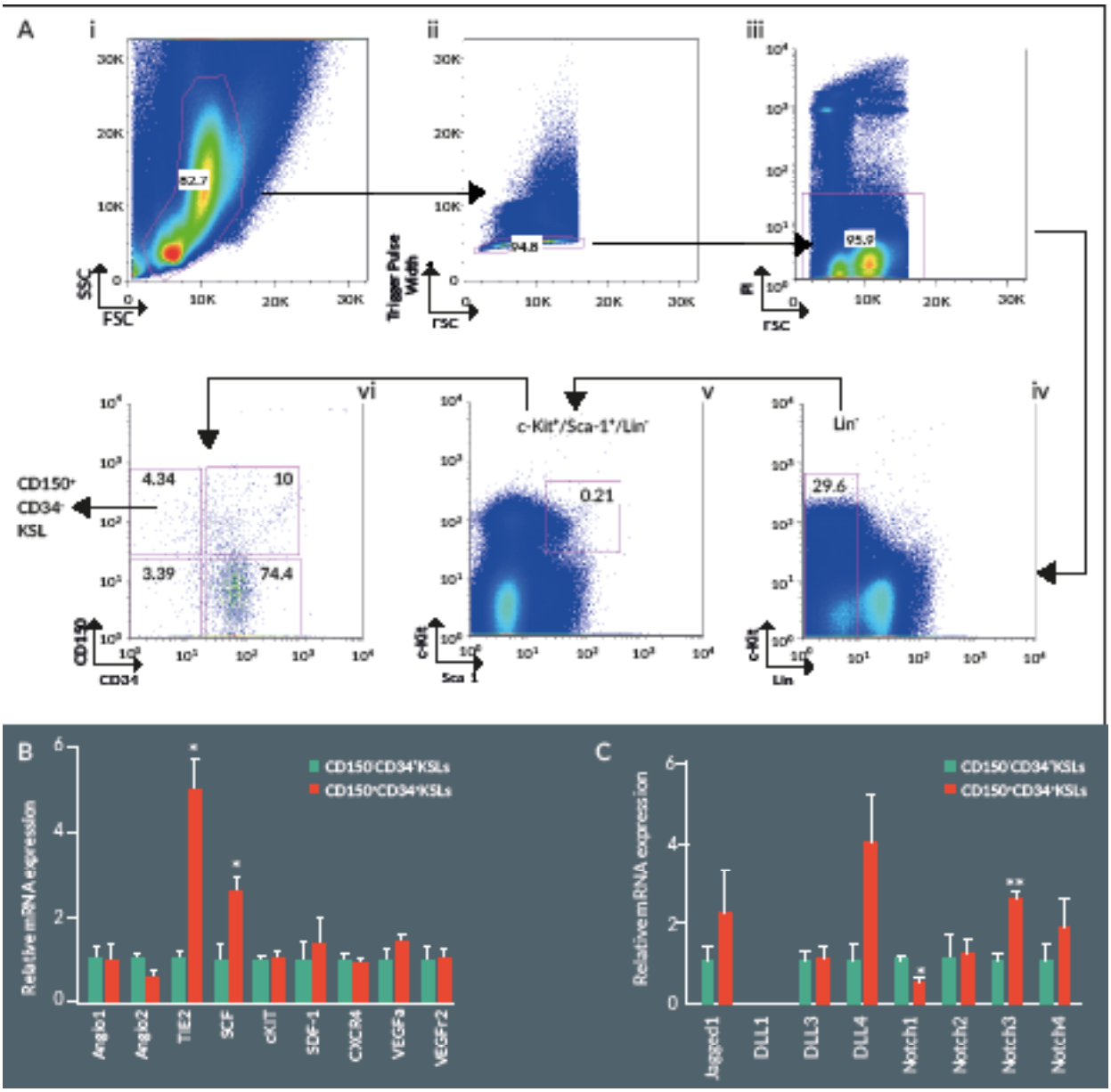

(**A**) Gating strategy for identification and sorting of CD150^{+}/CD34^{-} KSL cells. Total BM mononuclear fraction (i) were analyzed in a single cell gate in order to avoid aggregates (ii) and stained with propidium iodide to establish viable cells (iii). Lineage negative mononuclear cells (iv) were gated according to Sca-1 and c-Kit expression (v) and then CD150 positive cells were identified within the CD34 negative fraction (vi). (**B**) Expression of chemokines, stemness markers and angiogenic factors/receptors in the two fractions. (**C**) Expression of components of the Notch signaling pathway in the CD150 positive and CD150 negative CD34^{-} KSL fractions. Data are expressed as mean±SEM from three independent experiments. *P<0.05 and **P<0.01 vs. CD150 negative fraction.

DOI: 10.18609/cgti.2016.019

differentiation. Expressional analysis indicates higher levels of Notch3 and lower levels of Notch1 in the CD150^{+} fraction of CD34^{-}/KSL cells (Figure 1C).

Low dosage CD150^{+}/CD34^{-}/KSL cell therapy improves hemodynamic recovery & reparative angiogenesis in a mouse model of hindlimb ischemia

Preclinical cell therapy trials using total or fractioned BM cells showed the requirement of large dosages, generally exceeding 1 x 10^{6}, to successfully improve hemodynamic recovery in mice with operative limb ischemia [16,19]. Importantly, an amount of 5x10^{3} of KSL cells was able to achieve a similar improvement in functional neovascularization, thus suggesting that this cell population is greatly enriched for therapeutic angiogenic properties when compared to total BM cells [20]. In order to further define the truly salutary fraction within the bulk BM cell population, we performed a cell therapy

FIGURE 2A–B

Low dosage CD150^{+}/CD34^{-}/KSL cell therapy improves hemodynamic recovery and reparative neovascularization in a mouse model of hindlimb ischemia.

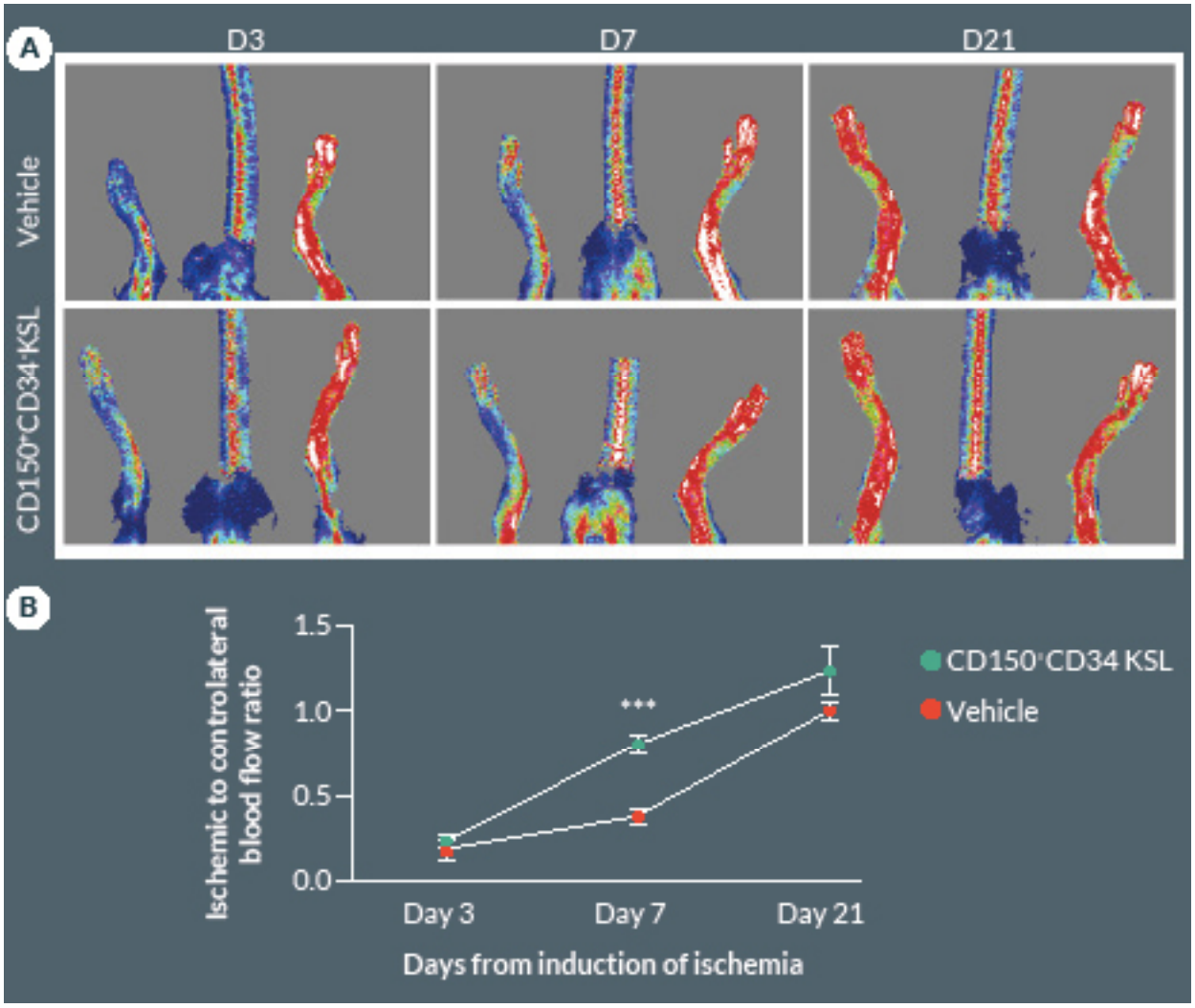

(A) Representative images of Laser Doppler blood flow captured during the follow up of vehicle- or CD150^{+}/CD34^{-} KSL cell-injected mice. (B) Line graph showing ischemic to contralateral blood flow ratio in the two groups.

FIGURE 2C–F

Low dosage CD150⁺/CD34⁻/KSL cell therapy improves hemodynamic recovery and reparative neovascularization in a mouse model of hindlimb ischemia.

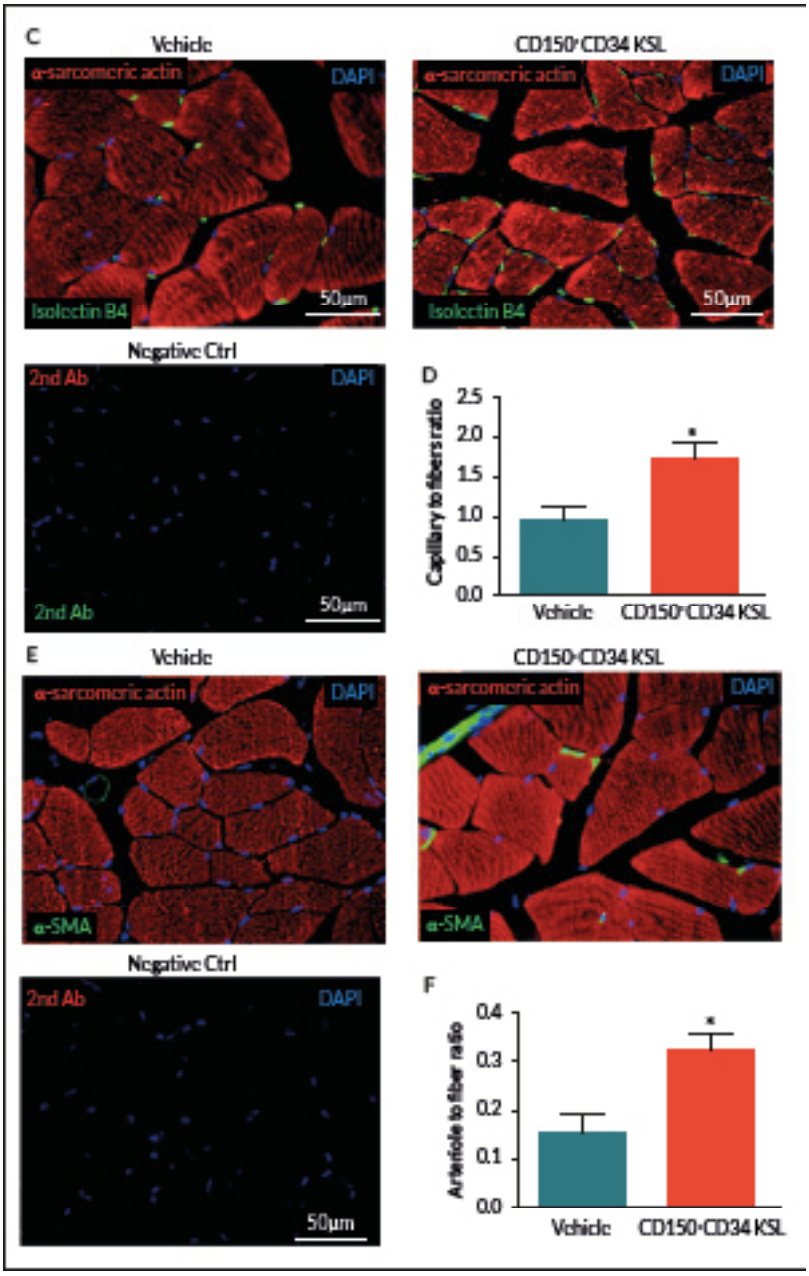

(C&D) Representative fluorescent microscopy images and bar graphs showing capillary staining **(C)** and counts **(D)**. Isolectin B4 is shown in green and α-sarcomeric actin in red. Nuclei are counterstained in blue by DAPI. **(E&F)** Representative fluorescent microscopy images and bar graphs showing arterioles staining **(E)** and counts **(F)**. Isolectin B4 is shown in green and α-SMA in red. Nuclei are counterstained in blue by DAPI. Data are expressed as mean ± SEM, *P<0.05 and ***P<0.001 vs. vehicle group (n = 6).

study using a very low dosage of CD150⁺CD34⁻ KSL cells. Results indicate that intra-muscular injection of 2 x 10^3 cells produces a significant acceleration in blood flow recovery as compared with vehicle ($P < 0.05$, Figure 2 A & B). Additionally, CD150⁺CD34⁻ KSL cell therapy increased the density of isolectin B4-positive capillaries (Figure 2 C & D) and α-SMA-positive arterioles (Figure 2 E & F). However, we could not detect any GFP⁺ injected cells in the adductor muscles at 21 days, thus suggesting the neovascularization benefit is mediated by paracrine mechanisms. Additionally, we found that CD150⁺CD34⁻ KSL cell therapy reduces the apoptosis of resident endothelial cells (Figure 3A & B) while increasing cell proliferation (Figure 3 C & D).

Clonogenic expansion of single CD150⁺CD34⁻ KSL cells

Having demonstrated that CD150⁺CD34⁻ KSL cell therapy is effective at a very low dosage, we next focused on the possibility of further restricting cell heterogeneity and eventually capturing the cell clone(s) responsible for the improvement of post-ischemic outcomes. To this end, we performed a single cell sorting of the CD150⁺CD34⁻ KSL population, followed by clonogenic expansion. Single-sorted cells were cultured for 2 weeks in methylcellulose medium M3236 supplemented with growth factors, such as SCF, VEGF, IL3, EGF, IGF-1, as previously described by Tanaka *et al* [17]. Under these conditions, sorted cells from three independent experiments formed colonies with a frequency of 8 ± 1%, with an average colony size of 22,083 ± 1,007 cells in 2 weeks (Figure 4A).

Successfully cultured CD150⁺CD34⁻ KSL cells were then characterized by flow cytometry

DOI: 10.18609/cgti.2016.019

FIGURE 3A–B

Low dosage CD150^{+}/CD34^{-}/KSL cell therapy improves the viability and proliferation of resident endothelial cells.

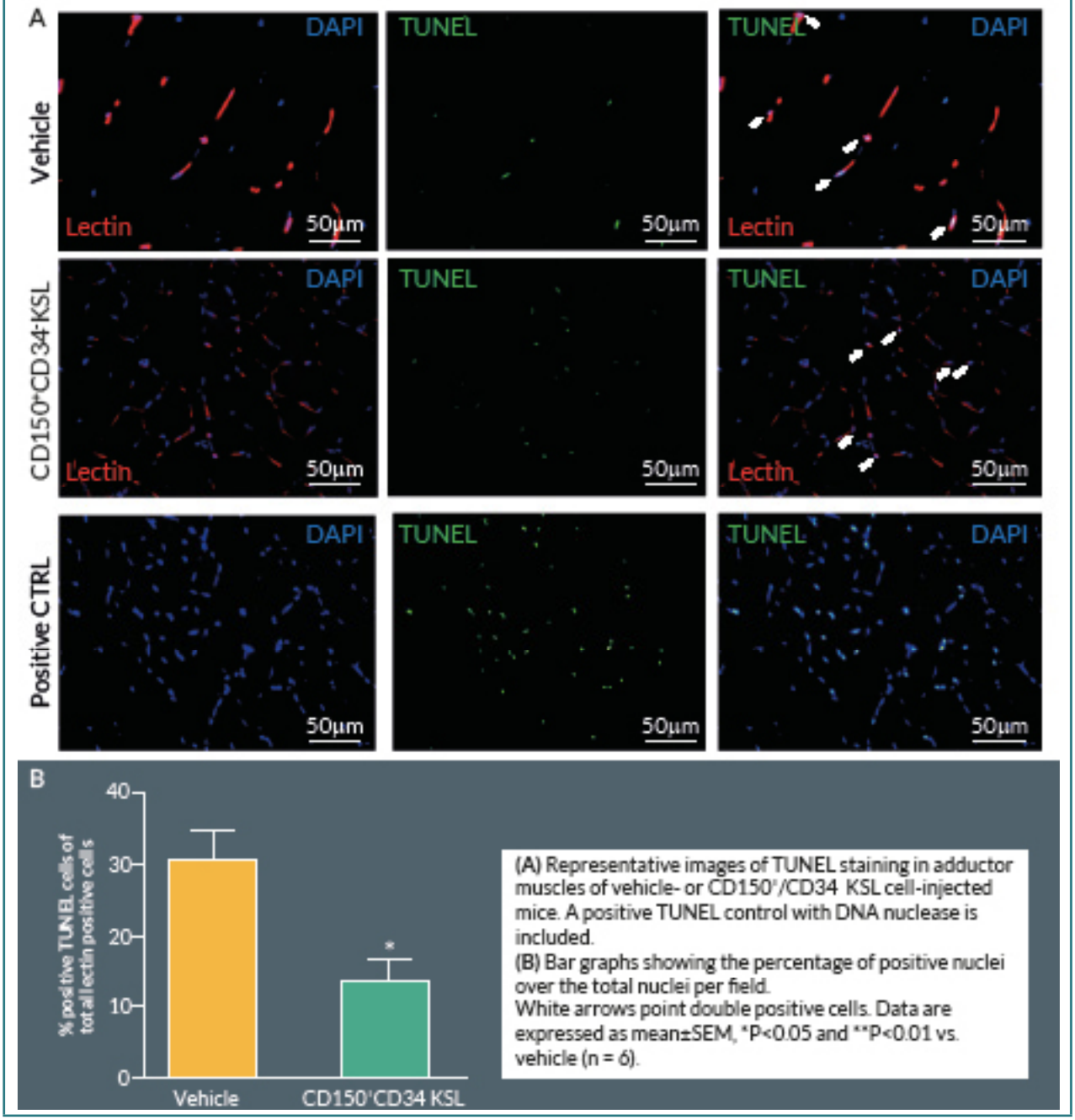

(A) Representative images of TUNEL staining in adductor muscles of vehicle- or CD150^{+}/CD34^{-} KSL cell-injected mice. A positive TUNEL control with DNA nuclease is included.
(B) Bar graphs showing the percentage of positive nuclei over the total nuclei per field.
White arrows point double positive cells. Data are expressed as mean±SEM, *P<0.05 and **P<0.01 vs. vehicle (n = 6).

to assess endothelial and progenitor markers. Clonogenic cells were positive for CD31 (54 ± 3%), c-Kit (37 ± 2%) and to a lower extent for Flk1 (16 ± 2%) and Tie2 (12 ± 1%) (Figure 4B). Previous investigations indicate that CD31 is a unique marker of a full spectrum of non-endothelial hematopoietic BM cells that are tightly associated with neovascularization [19,21]. In our study, CD31 was variably expressed among different colonies emerging from single sorted CD150^{+}CD34^{-} KSL cells. In order to characterize specific features associated with the relative abundance of CD31 antigen, we performed additional

FIGURE 3C–D

Low dosage CD150⁺/CD34⁻/KSL cell therapy improves the viability and proliferation of resident endothelial cells.

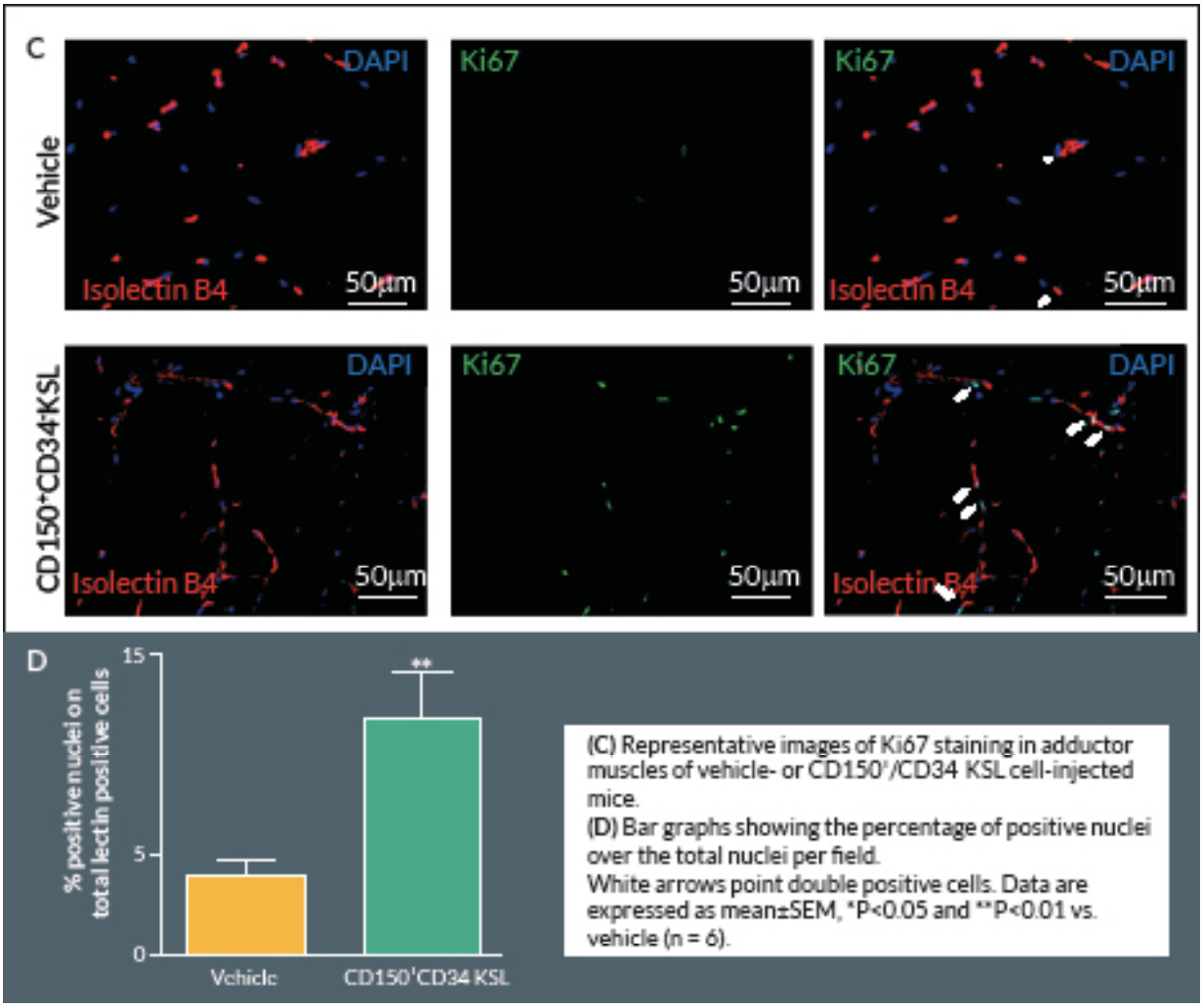

(C) Representative images of Ki67 staining in adductor muscles of vehicle- or CD150⁺/CD34 KSL cell-injected mice.
(D) Bar graphs showing the percentage of positive nuclei over the total nuclei per field.
White arrows point double positive cells. Data are expressed as mean±SEM, *P<0.05 and **P<0.01 vs. vehicle (n = 6).

expressional and *in vivo* studies comparing CD31^{high} and CD31^{low} colonies (Figure 4C). Flow cytometry indicate CD31^{high} colonies tend to have higher expression levels of c-Kit, Flk-1 and Tie-2 although these difference did not statistical significance (Figure 4D), Restricting comparative analyses to the CD31^{+} sub-fraction within CD31^{high} and CD31^{low} colonies, we found that c-Kit is 2-fold more abundant in the former ($P < 0.01$ vs CD31^{low}) (Figure 4D). Additional diversities were found at mRNA level with regard to the Notch signaling pathway, being DLL4 and Notch3 upregulated and Notch 2 downregulated in CD31^{high} as compared with CD31^{low} colonies (Figure 4E). Furthermore, the CD31^{high} population showed an upregulated expression of SCF and Tie2, whereas CXCR4 was downregulated (Figure 4F).

CD31^{high} cells improve hemodynamic recovery & reparative angiogenesis

Next we compared CD31^{high} and CD31^{low} cells vs. vehicle in the hindlimb ischemia model. We repeated the single cell sorting of the

DOI: 10.18609/cgti.2016.019

FIGURE 4

Clonogenic expansion of single CD150⁺CD34⁻ KSL cells.

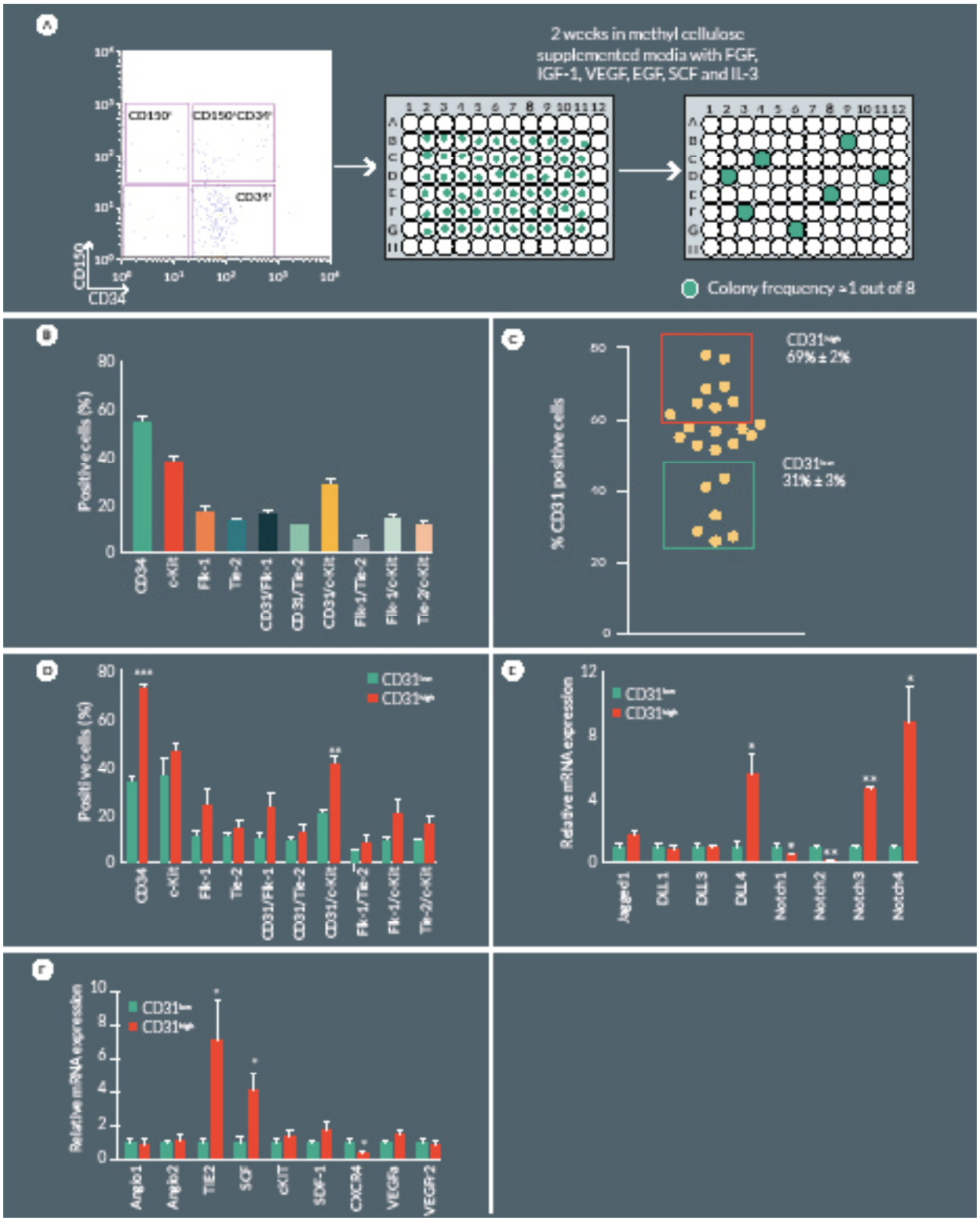

(A) CD150⁺/CD34⁻ KSL cells were single sorted in a 96 well plate EPC-CFA system based on methyl cellulose containing M3236 medium supplemented with 20 ng/ml SCF, 50ng/ml VEGF, 20 ng/ml IL-3, 50ng/ml EGF, 50 ng/ml IGF-1, and 2 U/ml heparin which allows improved expansion of colonies. Emerging colonies were harvested and analysed by flow cytometry and qPCR. **(B)** Bar graphs representing FACS analysis of all obtained colonies after 2 weeks of culture. **(C)** Scatter plot of the different colonies based on the percentage of CD31-positive cells in each colony established by FACS. Two distinct cluster of populations named CD31^{low} and CD31^{high} are highlighted. **(D)** Bar graph representing FACS data of surface antigen expression in the CD31^{low} and CD31^{high} populations. **(E-F)** Bar graphs showing qPCR data run on CD31^{low} and CD31^{high} single expanded CD150⁺CD34⁻ KSLs. Notch related and angiocrine factors gene expression of CD31^{high} cell group are expressed as fold change of the CD31^{low} cell group. Data from three independent experiments are expressed as mean±SEM. * P<0.05, **P <0.01 and ***P<0.001 vs. CD31^{low} group.

FIGURE 5A–D

Low dosage CD31^{high} cell therapy improves hemodynamic recovery and reparative neovascularization.

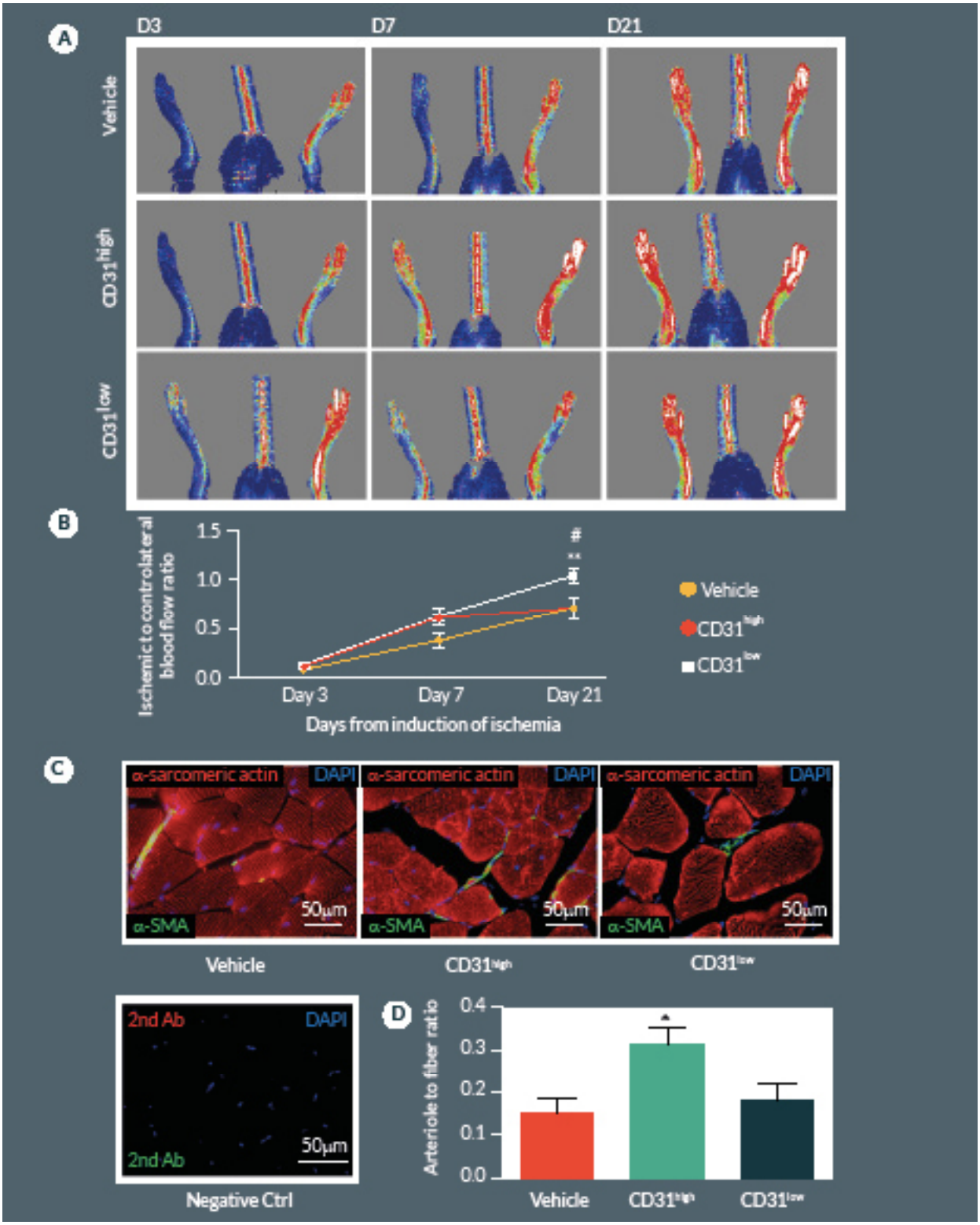

(**A**) Representative images of Laser Doppler blood flow recovery in mice injected with vehicle or clonogenically expanded CD31^{high} and CD31^{low} cells. (**B**) Line graphs showing ischemic to contralateral blood flow ratio in mice injected with vehicle, CD31^{high} or CD31^{low} cells. (**C-F**) Representative fluorescent microscopy image and bar graphs showing capillary (**C&D**) and arteriole density (**E&F**). Data are expressed as mean±SEM, *P<0.05, and **P<0.01 vs. vehicle group, #P<0.05 CD31^{high} vs. CD31^{low} group (n = 5).

DOI: 10.18609/cgti.2016.019

FIGURE 5E–F

Low dosage CD31^{high} cell therapy improves hemodynamic recovery and reparative neovascularization.

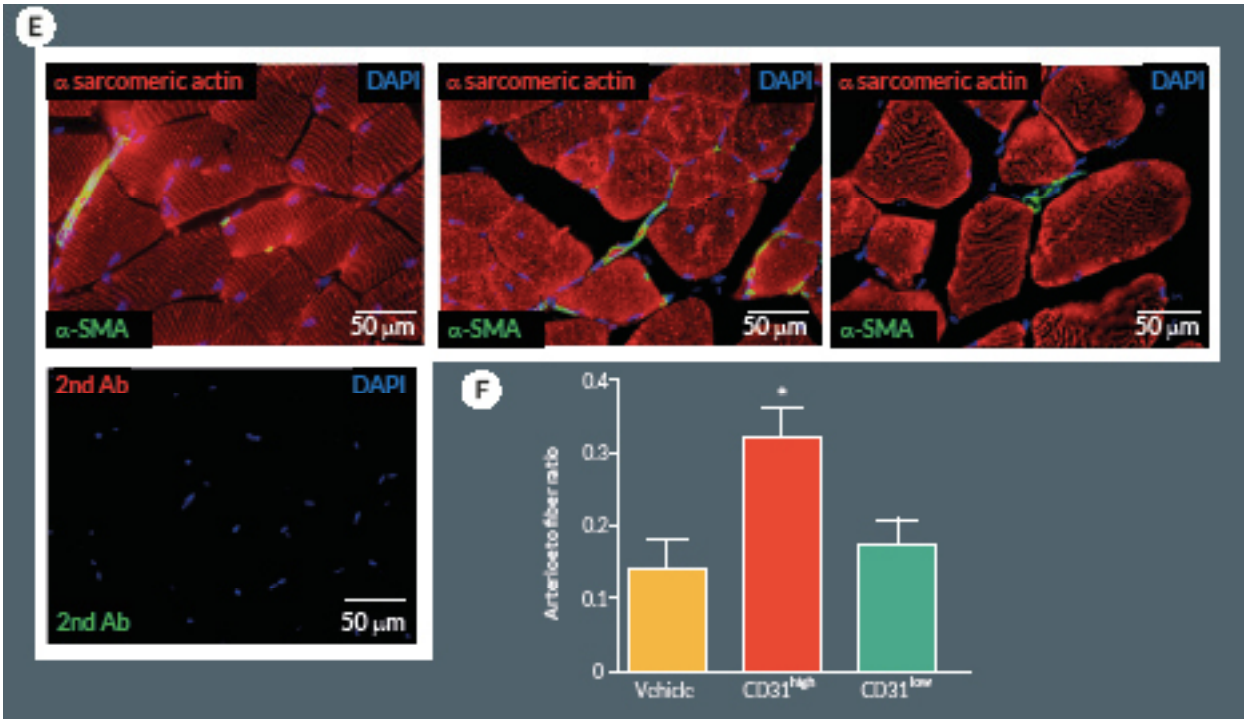

(**A**) Representative images of Laser Doppler blood flow recovery in mice injected with vehicle or clonogenically expanded CD31^{high} and CD31^{low} cells. (**B**) Line graphs showing ischemic to contralateral blood flow ratio in mice injected with vehicle, CD31^{high} or CD31^{low} cells. (**C-F**) Representative fluorescent microscopy image and bar graphs showing capillary (**C&D**) and arteriole density (**E&F**). Data are expressed as mean±SEM, *P<0.05, and **P<0.01 vs. vehicle group, #P<0.05 CD31^{high} vs. CD31^{low} group (n = 5).

CD150^{+}CD34^{-} KSL population obtaining four different clones (Supplemental Figure 1A). We selected the highest and the lowest CD31 expressing clones (99.3 and 19.8% respectively) containing enough cells to perform cell therapy in biological replicates. Flow cytometry analysis of antigen co-expression indicates the relative enrichment of Flk-1 and c-Kit in the CD31^{high} clone (Supplemental Figure 1B-D). Results of *in vivo* experiments are illustrated in Figure 5. Two-way ANOVA with repeated measurements identified an effect of time ($P < 0.001$) and cell treatment ($P < 0.01$) on blood flow recovery. Post-hoc analysis indicates that transplantation of CD31^{high} cells derived from clonogenic CD150^{+}CD34^{-} KSL cells is able to induce a complete hemodynamic recovery at day 21. On the other hand, CD31^{low} cells exerted only a transitory improvement in blood flow recovery at day 7, but failed to provide any additional beneficial effect over vehicle at day 21 (Figure 5A & B). In addition, the CD31^{high} cell population improved reparative angiogenesis in the ischemic muscles at capillary (Figure 5C & D) and arteriole level (Figure 5E & F) as compared with CD31^{low} cells or vehicle. Additionally, only mice injected with the CD31^{high} population retained the ability to decrease apoptosis (Figure 6A & B). Similarly, the CD31^{high} group showed a significant increase in proliferation compared with the CD31^{low} or vehicle groups (Figure 6C & D).

FIGURE 6A–B

Low dosage CD150⁺/CD34⁻/KSL cell therapy improves the viability and proliferation of resident endothelial cells.

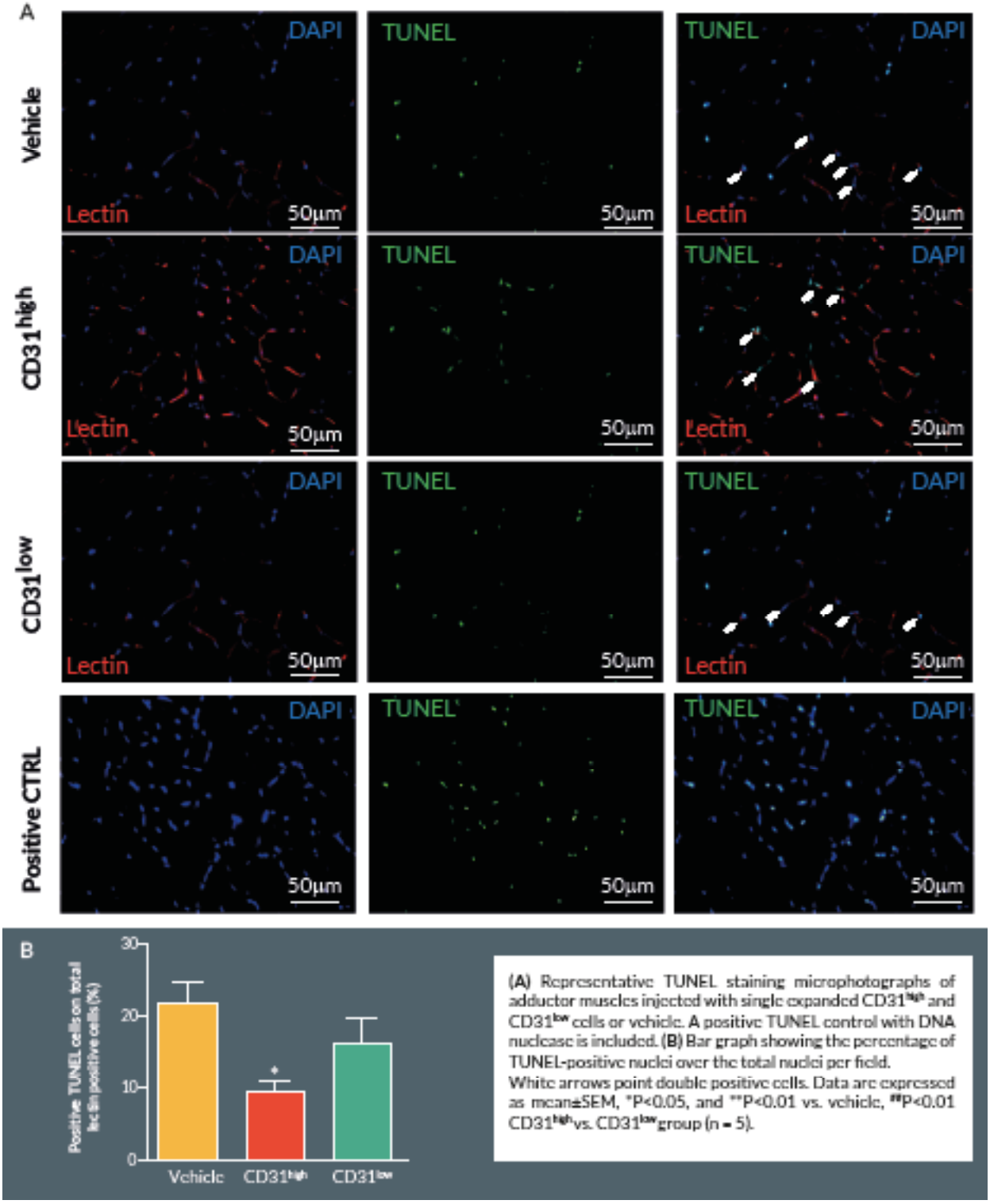

(A) Representative TUNEL staining microphotographs of adductor muscles injected with single expanded $CD31^{high}$ and $CD31^{low}$ cells or vehicle. A positive TUNEL control with DNA nuclease is included. (B) Bar graph showing the percentage of TUNEL-positive nuclei over the total nuclei per field. White arrows point double positive cells. Data are expressed as mean±SEM, *P<0.05, and **P<0.01 vs. vehicle, ##P<0.01 $CD31^{high}$ vs. $CD31^{low}$ group (n = 5).

DISCUSSION

This study demonstrates that a SLAM marker previously used to define the hierarchy of murine HSCs helps to distinguish truly pro-angiogenic elements within the total BM cell population. Furthermore, within $CD150^{+}CD34^{-}$ KSL

DOI: 10.18609/cgti.2016.019

FIGURE 6C–D

Low dosage CD150^{+}/CD34^{-}/KSL cell therapy improves the viability and proliferation of resident endothelial cells.

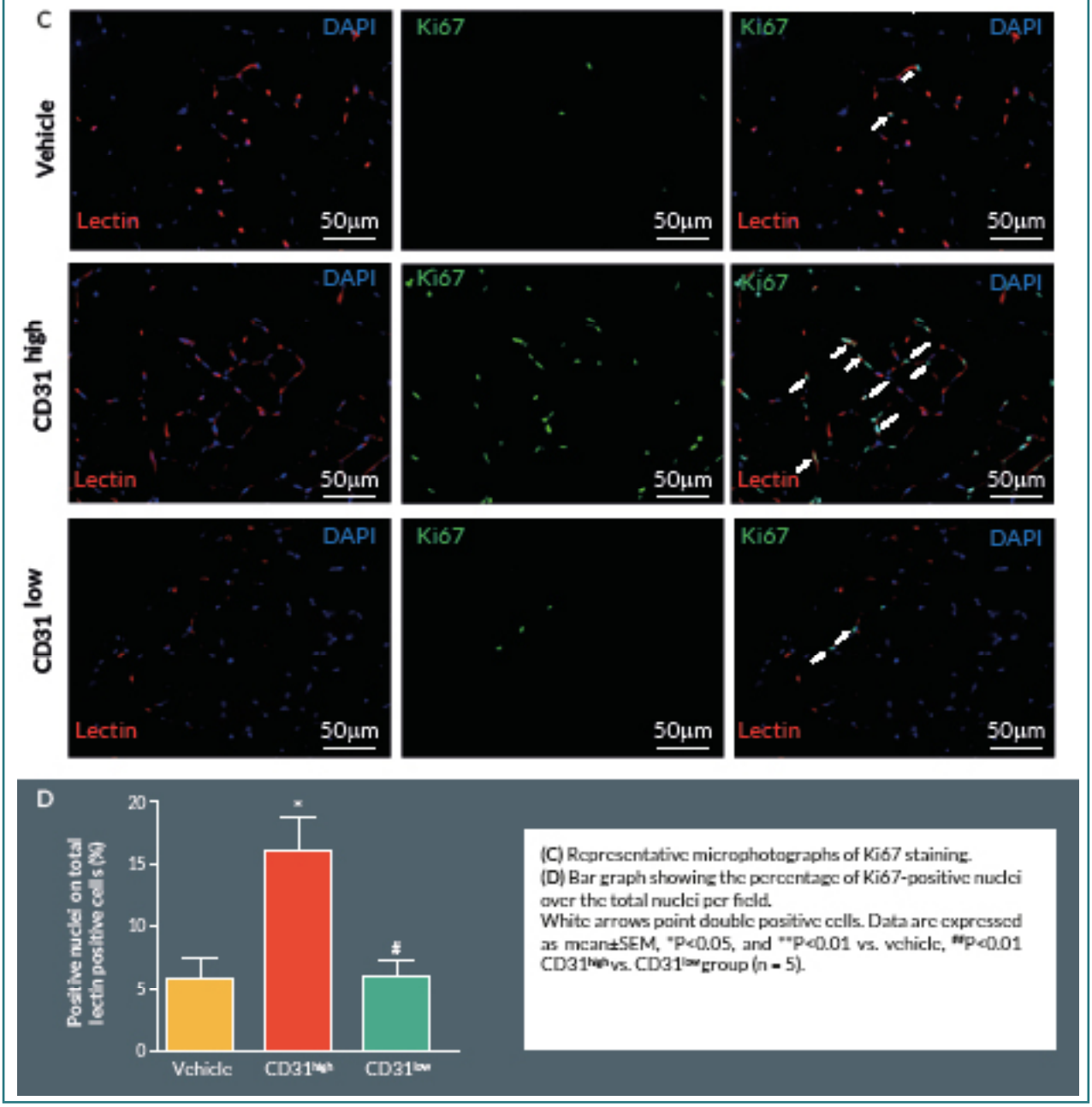

(C) Representative microphotographs of Ki67 staining. (D) Bar graph showing the percentage of Ki67-positive nuclei over the total nuclei per field. White arrows point double positive cells. Data are expressed as mean±SEM, *P<0.05, and **P<0.01 vs. vehicle, #P<0.01 CD31^{high} vs. CD31^{low} group (n = 5).

cells, we discovered that clonogenic cells expressing high levels of the CD31 antigen constitute the prevalent active component for stimulation of reparative angiogenesis *in vivo*.

Transplantation of BM-derived cells, including mononuclear cells, bona fide endothelial progenitor cells, mesenchymal stem cells, and HSCs were reported to promote therapeutic neovascularization in ischemic tissues. However, there are controversies in the field. In particular, unselected BM cells may comprise active as well as neutral and even counter-productive components, which may expose the recipient to adverse events including calcification, vascular plaque growth,

and worsening of tissue ischemia [22–24]. To make matters even more complicated, patients carrying multiple cardiovascular risk factors, i.e., the subjects who would most benefit from cell therapy, possess fewer and dysfunctional PACs. Hence, methodological improvements are still required to achieve optimization of PAC manufacture. Two main approaches have been used so far to isolate PACs from BM cells:

1. Culture and colony assays; and
2. Selection based on surface markers [reviewed in 25,26].

However, both methods have been criticized for not being an ideal source of quality-assured cell products. Hybrid approaches based on two-step separation by immunomagnetic sorting for stemness markers followed by chemokine-directed migration have been proposed to obtain antigenically-defined sub-fractions with intact functional qualities [27].

Here we report an additional attempt to identify PACs from the primitive population of LT-HSCs. The first important outcome of this investigation is that transplantation of $CD150^{+}CD34^{-}$ KSL cells provides robust stimulation of reparative angiogenesis in a mouse model of limb ischemia. The therapeutic effect is seemingly mediated by paracrine actions of injected cells as they could not be detected in the recipient muscle by use of a fluorescent marker. The second major result consists of the novel identification of clonogenic $CD150^{+}CD34^{-}$ KSL cells expressing abundant levels of CD31 as the active component responsible for therapeutic effects in the hindlimb ischemia model. CD31, also known as platelet endothelial cell adhesion molecule 1, is a 130-kDa cell surface molecule and a member of the immunoglobulin superfamily. It reportedly plays important roles in leukocyte migration, cell–cell adhesion, and anti-apoptotic signalling [28,29]. It is noteworthy that recent studies have designated CD31 as a novel marker to identify murine and human PACs for the treatment of ischemic cardiovascular disease [19,21]. The above investigations indicate that CD31 is almost universally expressed among different BM cells and that both $CD31^{+}Lin^{+}$ or $CD31^{+}Lin^{-}$ cells perform equally well in improving the recovery of ischemic limbs, suggesting that both mature and immature BM cells may be instrumental to tissue healing [19,21]. Our investigation applies the use of the CD31 marker to clonogenic cells derived from multipotent LT-HSCs, thereby allowing purification of the definitive cell product within the primitive fraction of BM cells. In agreement with previous studies, CD31 was expressed by multi-potent LT-HSCs [19,21]. Unexpectedly however, we found a wide variability in the abundance of this surface antigen among different clones. Most importantly, *in vivo* studies show a clear association between the abundance of CD31 and therapeutic activity, with $CD31^{high}/CD150^{+}CD34^{-}$ KSL cells exerting more complete and prolonged recovery from ischemia as compared with $CD31^{low}/CD150^{+}CD34^{-}$ KSL cells. Importantly, transplantation of clonogenic $CD31^{high}/CD150^{+}CD34^{-}$ KSL cells also resulted in salutary effects on viability and proliferation of resident vascular cells.

The Notch signalling pathway regulates multiple aspects of hematopoiesis. *Ex vivo* exposure of

DOI: 10.18609/cgti.2016.019

mouse or human HSCs to Notch ligands was shown to enhance cytokine-mediated expansion, leading to preclinical testing and early clinical trials using Notch-expanded progenitors to boost hematopoietic recovery [30]. However, whether Notch regulates PAC expansion and function remains unknown. Our preliminary data on gene expression identify a differential pattern in Notch components between the two clonogenic populations expressing high or low CD31 levels. Intriguingly, DDL4 was upregulated in $CD31^{high}/CD150^{+}CD34^{-}$ KSL cells. We have previously reported that an intact DDL4 signalling is essential for proper angiogenesis and recruitment of circulating cells along nascent vessels [31]. Likewise, we found $CD31^{high}/CD150^{+}CD34^{-}$ KSL cells express higher levels of Tie2, an angiopoietin receptor implicated in the development of definitive hematopoiesis and angiogenesis [32]. Further studies are necessary to understand the relevance of these expressional difference in relation to therapeutic outcomes of $CD31^{high}$ and $CD31^{low}$ cells.

In conclusion, the present study highlights the benefit of a purified population of primitive HSCs for the treatment of limb ischemia. Translation of the approach to human BMs could lead to the significant enhancement of current cell therapies for cardiovascular disease.

ACKNOWLEDGEMENTS

We are thankful to the Flow Cytometry facility at the University of Bristol and to Dir. Andrew Herman. This study was funded by BHF program grant "Unravelling mechanisms of stem cell depletion for preservation of regenerative fitness in patients with diabetes".

ETHICAL CONDUCT OF RESEARCH

The authors state that they have obtained appropriate institutional review board approval or have followed the principles outlined in the Declaration of Helsinki for all human or animal experimental investigations. In addition, for investigations involving human subjects, informed consent has been obtained from the participants involved.

FINANCIAL & COMPETING INTERESTS DISCLOSURE

The authors have no relevant financial involvement with an organization or entity with a financial interest in or financial conflict with the subject matter or materials discussed in the manuscript. This includes employment, consultancies, honoraria, stock options or ownership, expert testimony, grants or patents received or pending, or royalties.

No writing assistance was utilized in the production of this manuscript.

REFERENCES

1. Hiatt WR. Medical treatment of peripheral arterial disease and claudication. *N. Engl. J Med.* 2001; 344, 1608–21.
2. Faglia E, Clerici G, Losa S *et al.* Limb revascularization feasibility in diabetic patients with critical limb ischemia: results from a cohort of 344 consecutive unselected diabetic patients evaluated in 2009. *Diabetes Res. Clin. Pract.* 2012; 95, 364–71.
3. Spinetti G, Specchia C, Fortunato O *et al.* Migratory activity of circulating mononuclear cells is associated with cardiovascular mortality in type 2 diabetic patients with critical limb

ischemia. *Diabetes Care* 2014; 37, 1410–7.

4. Tongers J, Roncalli JG and Losordo DW. Therapeutic angiogenesis for critical limb ischemia: microvascular therapies coming of age. *Circulation* 2008; 118, 9–16.
5. Matoba S, Tatsumi T, Murohara T *et al*. Long-term clinical outcome after intramuscular implantation of bone marrow mononuclear cells (Therapeutic Angiogenesis by Cell Transplantation [TACT] trial) in patients with chronic limb ischemia. *Am. Heart J*. 2008; 156, 1010–8.
6. Takahashi T, Kalka C, Masuda H *et al*. Ischemia- and cytokine-induced mobilization of bone marrow-derived endothelial progenitor cells for neovascularization. *Nat. Med*. 1999; 5, 434–8.
7. Kusumbe AP, Ramasamy SK, Adams RH. Coupling of angiogenesis and osteogenesis by a specific vessel subtype in bone. *Nature* 2014; 507, 323–8.
8. Ding BS, Nolan DJ, Butler JM *et al*. Inductive angiocrine signals from sinusoidal endothelium are required for liver regeneration. *Nature* 2010; 468, 310–5.
9. Ellis SL, Grassinger J, Jones A *et al*. The relationship between bone, hemopoietic stem cells, and vasculature. *Blood* 2011; 118, 1516–24.
10. Sacchetti B, Funari A, Michienzi S *et al*. Self-renewing osteoprogenitors in bone marrow sinusoids can organize a hematopoietic microenvironment. *Cell* 2007; 131, 324–36.
11. Corselli M, Chin CJ, Parekh C *et al*. Perivascular support of human hematopoietic stem/progenitor cells. *Blood* 2013; 121, 2891–901.
12. Sahoo S, Klychko E, Thorne T *et al*. Exosomes from human CD34(+) stem cells mediate their proangiogenic paracrine activity. *Circ. Res.* 2011; 109, 724–8.
13. Kumar AH, Metharom P, Schmeckpeper J, Weiss S, Martin K, Caplice NM. Bone marrow-derived CX3CR1 progenitors contribute to neointimal smooth muscle cells via fractalkine CX3CR1 interaction. *FASEB J*. 2010; 24, 81–92.
14. Morita Y, Ema H, Nakauchi H. Heterogeneity and hierarchy within the most primitive hematopoietic stem cell compartment. *J. Exp. Med.* 2010; 207, 1173–82.
15. Kiel MJ, Yilmaz OH, Iwashita T, Yilmaz OH, Terhorst C, Morrison SJ. SLAM family receptors distinguish hematopoietic stem and progenitor cells and reveal endothelial niches for stem cells. *Cell* 2005; 121, 1109–21.
16. Sugihara S, Yamamoto Y, Matsuura T *et al*. Age-related BM-MNC dysfunction hampers neovascularization. *Mech. Ageing* Dev. 2007; 128, 511–6.
17. Tanaka R, Wada M, Kwon SM *et al*. The effects of flap ischemia on normal and diabetic progenitor cell function. *Plast. Reconstr. Surg*. 2008; 121, 1929–42.
18. Kwon SM, Eguchi M, Wada M *et al*. Specific Jagged-1 signal from bone marrow microenvironment is required for endothelial progenitor cell development for neovascularization. *Circulation* 2008; 118, 157–65.
19. Kim H, Cho HJ, Kim SW *et al*. CD31+ cells represent highly angiogenic and vasculogenic cells in bone marrow: novel role of nonendothelial CD31+ cells in neovascularization and their therapeutic effects on ischemic vascular disease. *Circ. Res.* 2010; 107, 602–14.
20. Kwon SM, Lee YK, Yokoyama A *et al*. Differential activity of bone marrow hematopoietic stem cell subpopulations for EPC development and ischemic neovascularization. *J. Mol. Cell. Cardiol*. 2011; 51, 308–17.
21. Kim SW, Kim H, Cho HJ, Lee JU, Levit R, Yoon YS. Human peripheral blood-derived CD31+ cells have robust angiogenic and vasculogenic properties and are effective for treating ischemic vascular disease. *J. Am. Coll. Cardiol*. 2010; 56, 593–607.
22. Yoon YS, Park JS, Tkebuchava T, Luedeman C, Losordo DW. Unexpected severe calcification after transplantation of bone marrow cells in acute myocardial infarction. *Circulation*. 2004; 109, 3154–7.
23. George J, Afek A, Abashidze A *et al*. Transfer of endothelial progenitor and bone marrow cells influences atherosclerotic plaque size and composition in apolipoprotein E knockout mice. *Arterioscler. Thromb. Vasc. Biol*. 2005; 25, 2636–41.
24. Ziegelhoeffer T, Fernandez B, Kostin S, Heil M, Voswinckel R, Helisch A, Schaper W. Bone marrow-derived cells do not incorporate into the adult growing vasculature. *Circ. Res.* 2004; 94, 230–8.
25. Timmermans F, Plum J, Yoder MC, Ingram DA, Vandekerckhove B, Case J. Endothelial progenitor cells: identity defined? *J. Cell. Mol. Med.* 2009; 13, 87–102.
26. Fadini GP, Losordo D, Dimmeler S. Critical reevaluation of endothelial progenitor cell phenotypes for therapeutic and diagnostic use. *Circ. Res.* 2012; 110, 624–37.
27. Ascione R, Rowlinson J, Avolio E *et al*. Migration towards SDF-1 selects angiogenin-expressing bone marrow monocytes endowed with cardiac reparative activity in patients with previous myocardial infarction. *J. Stem Cell Res. Ther*. 2015; 6, 53.
28. Baumann CI, Bailey AS, Li W, Ferkowicz MJ, Yoder MC, Fleming WH.

 DOI: 10.18609/cgti.2016.019

PECAM-1 is expressed on hematopoietic stem cells throughout ontogeny and identifies a population of erythroid progenitors. *Blood*. 2004; 104, 1010–6.

29. Woodfin A, Voisin MB and Nourshargh S. PECAM-1: a multi-functional molecule in inflammation and vascular biology. *Arterioscler. Thromb. Vasc. Biol.* 2007; 27, 2514–23.

30. Delaney C, Heimfeld S, Brashem-Stein C, Voorhies H, Manger RL, Bernstein ID. Notch-mediated expansion of human cord blood progenitor cells capable of rapid myeloid reconstitution. *Nat. Med*. 2010; 16, 232–6.

31. Al Haj Zen A, Oikawa A, Bazan-Peregrino M, Meloni M, Emanueli C, Madeddu P. Inhibition of delta-like-4-mediated signaling impairs reparative angiogenesis after ischemia. *Circ. Res*. 2010; 107, 283-93.

32. Takakura N, Huang XL, Naruse T *et al*. Critical role of the TIE2 endothelial cell receptor in the development of definitive hematopoiesis. *Immunity* 1998; 9, 677–86.

AFFILIATION

Corresponding Author:

Paolo Madeddu MD

Chair Experimental Cardiovascular Medicine, Bristol Heart Institute, University of Bristol, Level 7, Bristol Royal Infirmary, Upper Maudlin Street, Bristol, BS28HW, UK

Tel/Fax: +44 (0)1179 283904

Email: madeddu@yahoo.com